

## Optical second harmonic generation from the twin boundary of ZnO thin films grown on silicon

Kuang-Yao Lo, Shih-Chieh Lo, Chang-Feng Yu, Teddy Tite, Jung-Y. Huang, Yi-Jen Huang, Ren-Chuan Chang, and Sheng-Yuan Chu

Citation: *Applied Physics Letters* **92**, 091909 (2008); doi: 10.1063/1.2891334

View online: <http://dx.doi.org/10.1063/1.2891334>

View Table of Contents: <http://scitation.aip.org/content/aip/journal/apl/92/9?ver=pdfcov>

Published by the [AIP Publishing](#)

---

### Articles you may be interested in

[Characterization of the quality of ZnO thin films using reflective second harmonic generation](#)  
Appl. Phys. Lett. **95**, 091904 (2009); 10.1063/1.3216848

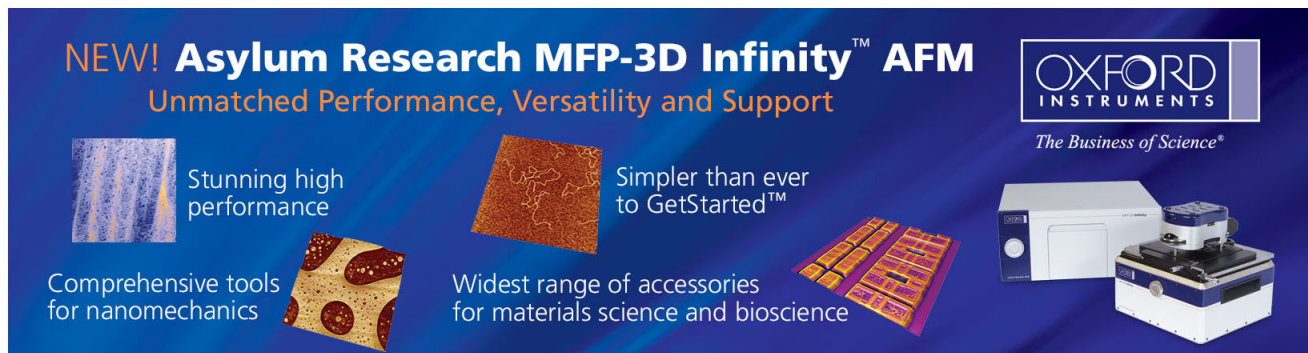
[Origin of second-order nonlinear optical response of polarity-controlled ZnO films](#)  
Appl. Phys. Lett. **94**, 231118 (2009); 10.1063/1.3152773

[Reflective second harmonic generation from ZnO thin films: A study on the Zn–O bonding](#)  
Appl. Phys. Lett. **90**, 161904 (2007); 10.1063/1.2723671

[Efficient third-harmonic generation in a thin nanocrystalline film of ZnO](#)  
Appl. Phys. Lett. **83**, 3993 (2003); 10.1063/1.1623948

[Large second harmonic response in ZnO thin films](#)  
Appl. Phys. Lett. **80**, 401 (2002); 10.1063/1.1435065

---

The advertisement features a dark blue background with white and orange text. At the top left, it says 'NEW! Asylum Research MFP-3D Infinity™ AFM' in large white letters, followed by 'Unmatched Performance, Versatility and Support' in orange. To the right is the Oxford Instruments logo with the tagline 'The Business of Science®'. Below the text are four images: a blue textured surface, a brown textured surface, a grid of small yellow and red squares, and a photograph of the MFP-3D Infinity AFM instrument. Text descriptions are placed around these images: 'Stunning high performance' next to the blue surface, 'Simpler than ever to GetStarted™' next to the brown surface, 'Comprehensive tools for nanomechanics' next to the grid, and 'Widest range of accessories for materials science and bioscience' next to the instrument photo.

## Optical second harmonic generation from the twin boundary of ZnO thin films grown on silicon

Kuang-Yao Lo,<sup>1,a)</sup> Shih-Chieh Lo,<sup>1</sup> Chang-Feng Yu,<sup>1</sup> Teddy Tite,<sup>1</sup> Jung-Y. Huang,<sup>2</sup> Yi-Jen Huang,<sup>3</sup> Ren-Chuan Chang,<sup>3</sup> and Sheng-Yuan Chu<sup>3</sup>

<sup>1</sup>Department of Applied Physics, National Chia Yi University, ChiaYi 600, Taiwan

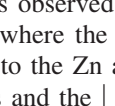
<sup>2</sup>Department of Photonics, National Chiao Tung University, Hsinchu 300, Taiwan

<sup>3</sup>Department of Electrical Engineering, National Cheng Kung University, Tainan 700, Taiwan

(Received 27 January 2008; accepted 7 February 2008; published online 6 March 2008)

The symmetry of the twin boundaries of ZnO epitaxial film was detected with reflective second harmonic generation (RSHG). The twin boundaries exhibit mirror symmetry with a polar configuration across the boundary plane and yield a nonvanishing polar contribution to RSHG. The nonvanishing second-order susceptibility supports the notion that the measured RSHG originates from the planar defect, which depends on the residual stress in the thin film. We analyzed our RSHG result by correlating the macroscopic data from optic probe with the microscopic data from tunneling electron microscope. © 2008 American Institute of Physics. [DOI: 10.1063/1.2891334]

Zinc oxide (ZnO) thin film has attracted considerable interest for its optical, electrical, and mechanical properties. Experimental and theoretical studies on ZnO crystals have revealed the presence of a giant permanent dipole moment, which yields a significant piezoelectric effect for a variety of micromechanical devices.<sup>1</sup> Zinc oxide is a wide direct band-gap (3.37 eV) II-VI semiconductor with large exciton binding energy (60 meV),<sup>2</sup> which have been shown to be valuable for short wavelength optoelectronic devices such as light emitting diodes and lasers. From the viewpoint of material synthesis, ZnO offers further advantages of low cost and no toxic chemicals involved in its synthesis.

ZnO films have been deposited with a variety of methods such as magnetron sputtering, pulsed laser deposition, or metal organic chemical vapor deposition (MOCVD).<sup>3,4</sup> The resulting films with single-crystal quality possess very high piezoelectric coefficients. It was found that a proper selection of substrate materials is crucial for yielding a high-quality ZnO film.<sup>5,6</sup> Silicon crystal has been widely used as the substrate for thin film deposition because of the large resources available in the highly matured silicon-based industry. However, the large discrepancy in the thermal expansion coefficients and lattice mismatch between ZnO film and Si substrate often produce a fairly large stress in the film. Moreover, extended defects such as twin boundaries were also observed in the wurtzite structure of ZnO thin films<sup>7,8</sup> with high-resolution Z-contrast transmission electron microscopy (TEM). The twin boundaries observed have the head-to-tail polar configuration  where the arrow indicates the polarity direction from the O to the Zn atoms along the O-Zn bonds parallel to the *c* axis and the | symbol denotes the twin-boundary plane.<sup>7</sup> The resulting twin boundaries exhibit mirror symmetry with the polar configuration providing a nonvanishing contribution to the second-order nonlinear optical susceptibility, which allows the polar structure to be probed with optical second harmonic generation (SHG) technique.

Reflective SHG (RSHG) has been developed into a versatile probe for thin film, surface, and interfacial studies.<sup>9,10</sup>

It has been widely used for the process control of thin film deposition and the rapid thermal annealing of ion implantation.<sup>11,12</sup> Rotational anisotropy SHG (RA-SHG) provided useful information about the strained layer,<sup>13,14</sup> the quality of epitaxial films,<sup>15</sup> and the surface reconstruction.<sup>12</sup> It was found that misfit dislocation defects in an epitaxial film can affect the second-order nonlinear optical susceptibility  $\chi^{(2)}$ ; therefore, their presence shall be revealed with RA-SHG.<sup>16</sup>

In our previous study of ZnO thin films grown on the *c*-plane of sapphire by MOCVD, we found that the RSHG signal originated from the mirror symmetry of twin boundaries is mixed with the 3 mm symmetric RSHG pattern that is raised from the Zn-O bonding on the surface of a well-grown ZnO thin film.<sup>17</sup> However, the additional contribution with mirrorlike symmetry originated from the twin boundaries deserves to be investigated further for its potential application as an indicator of the film quality.

In this work, we studied RSHG of ZnO thin film grown on Si(111) substrate by sputtering. The resulting surfaces of ZnO thin films were not perfectly smooth to eliminate the RSHG contribution of 3 mm symmetry.<sup>17</sup> Since *s*-polarized RSHG excited by *s*-polarized fundamental light (*ss*-RSHG) is sensitive to the anisotropic contribution dominated by the symmetrical structure,<sup>18</sup> we therefore employed the *ss*-RSHG to probe the nonvanishing polarity of twin boundaries in a ZnO film. We analyzed our RSHG result by correlating the macroscopic data from optic probe with the microscopic data from TEM.

ZnO films were deposited from a ZnO target of 99.9% purity by using a magnetron sputtering system with a rf power of 60 W. Substrates used were *p*-type Si(111) (Boron dopant, 4–10  $\Omega$  cm), cleaned thoroughly with organic solvents and dried before loading in the sputtering system. The chamber was pumped down to  $6 \times 10^{-6}$  torr before introducing premixed Ar and O<sub>2</sub> gases into the chamber through a precision leak valve. The volume ratio of argon and oxygen was controlled to 1:1 by an electronic mass flow controller. The working pressure was kept at 3 mtorr. The ZnO films were deposited at the substrate temperatures of 100, 200, and 300 °C, respectively, for 3 h and naturally cooled down to room temperature. The x-ray diffraction (XRD) patterns of

<sup>a)</sup>Electronic mail: kuanglo@mail.nycu.edu.tw.

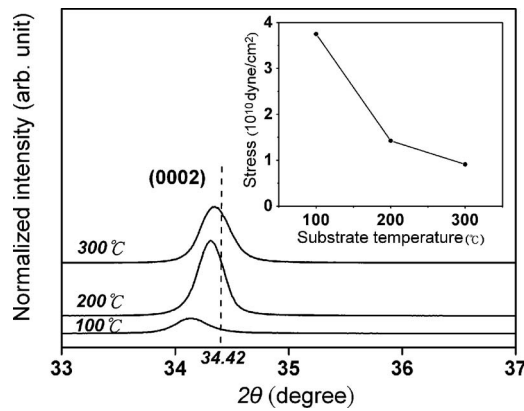


FIG. 1. The x-ray patterns of ZnO films deposited on Si(111) at different substrate temperature. The inset shows the stress calculated by the XRD profiles and peak shifts of the ZnO (0002) peak.

the resulting ZnO films on the Si(111) with different substrate temperatures were presented in the Fig. 1. Only one peak corresponding to the (0002) plane of ZnO crystal appears, suggesting these films to be preferentially deposited at a  $c$ -axis orientation. In some reported literatures, the strain of ZnO film was calculated by measuring the diffraction peak shift relative to that of bulk ZnO.<sup>19,20</sup> The inset of Fig. 1 shows the embedding stresses estimated by the above-mentioned method. The diffraction peak shift from the (0002) plane to the higher  $2\theta$  side indicates that the tensile strain in the film decreases with increasing substrate temperature.

The setup of SHG measurement was detailed in Ref. 12. During an azimuthal scan of the sample, the surface normal was aligned along the rotation axis and the excitation laser hit the rotational center to ensure the RSHG beam striking the cathode of photomultiplier tube at the same position. The  $ss$ -RSHG pattern of ZnO film grown on Si(111) substrate was shown in the Fig. 2.

The ZnO crystal prepared exhibits a wurtzite structure with 6 mm ( $C_{6v}$ ) symmetry. The second-order nonlinear op-

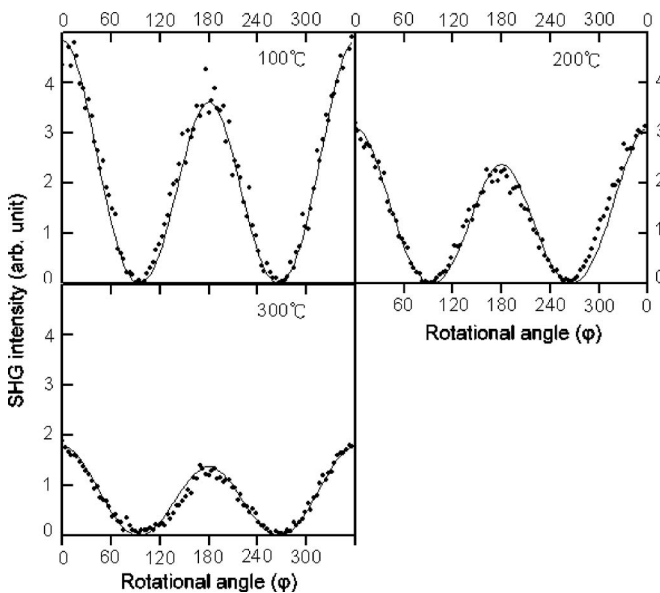


FIG. 2. The  $s$ -polarized RSHG pattern excited with  $s$ -polarized light acquired with a ZnO film on Si(111) substrate deposited at a temperature of 100, 200, and 300 °C.

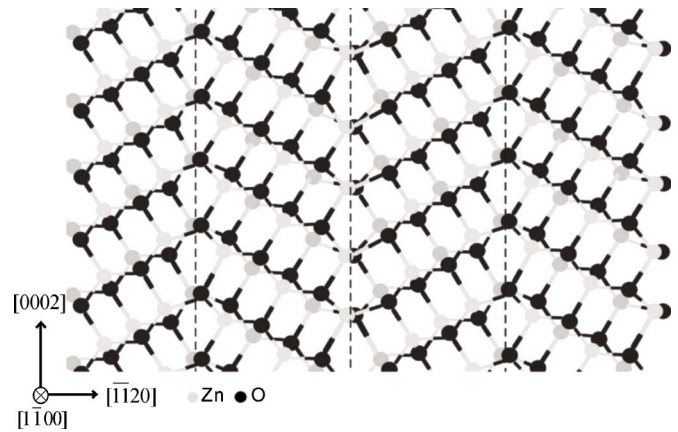


FIG. 3. (Color online) The arrow indicates the direction of the nonvanishing polarity from the O to the Zn atoms on the twin boundary. The dashed line denotes the  $[1\bar{1}00]/(1102)$  twin boundary in ZnO along the  $[1\bar{1}00]$  zone axis (Ref. 7).

tical susceptibility tensor is characterized by the following nonvanishing components  $\chi_{xzx}^{(2)} = \chi_{yyz}^{(2)} = \chi_{15}^{(2)}$ ,  $\chi_{zxx}^{(2)} = \chi_{zzy}^{(2)} = \chi_{31}^{(2)}$ , and  $\chi_{zzz}^{(2)} = \chi_{33}^{(2)}$ . There shall be no  $ss$ -RSHG signals from the ZnO bulk. Actually, the mirrorlike symmetrical patterns are shown in Fig. 2, in which there is no additional 3 mm symmetrical contribution raised from Zn–O bonding on the surface.<sup>17</sup>

ZnO (0002) layer with hexagonal wurtzite structure ( $a=3.249$  Å,  $c=5.207$  Å) can be epitaxially grown on silicon (111) substrate by matching the four silicon (220) planes with the five  $(11\bar{2}0)$  planes of ZnO. The spacing of ZnO  $(11\bar{2}0)$  planes ( $a/2=1.62$  Å) has about 40.1% strain with (220) planes of silicon.<sup>21</sup> As the deposited film exceeds the critical thickness, planar defects appear at the strained interface in order to relax the excess stress.<sup>22</sup> The planar defects could be a discontinuity of a perfect crystal structure across a plane, which contains grain boundaries, stacking faults, and twin boundaries.<sup>23</sup> In particular, a twin boundary is the regular growing together of crystals of the same sort, sharing some of the same crystal lattice with a mirror symmetry operation, which often occurs with crystal growth or through mechanical stress.<sup>23</sup> Yan *et al.* presented the atomic structure and the electronic effects of the  $[1\bar{1}00]/(11\bar{2}2)$  twin boundaries in wurtzite ZnO by using high-resolution  $Z$ -contrast TEM. The twin boundary was found to have the head-to-tail polarity configuration to avoid dangling bonds and yields fairly low twin-boundary energy of 0.040 J/m<sup>2</sup>. The polarity in the twin boundary exhibits a mirror symmetry across the boundary plane.<sup>7</sup>

The overall effect of these twin boundaries on the strained interface is a  $C_{1v}$  symmetry with a vertical mirror plane  $\sigma_v$  perpendicular to the  $x$  axis, which is the  $[11\bar{2}0]$  direction, as shown in Fig. 3.<sup>17</sup> Therefore, the nonvanishing second-order nonlinear optical susceptibility tensor components shall possess an even number of  $y$  subscript. The second-order susceptibility perturbed by the twin boundary leads to a nonvanishing  $ss$ -RSHG intensity,<sup>24</sup> which can be expressed as

$$I_{s \rightarrow s}^{(2),m} \propto |\cos \phi (\cos^2 \phi \chi_{xxx}^{(2),m} + 2 \sin^2 \phi \chi_{xyy}^{(2),m})|^2, \quad (1)$$

where  $\chi_{ijk}^{(2),m}$  is the component of the second-order susceptibility tensor with  $C_{1v}$  symmetry. In view that the  $ss$ -SHG

intensity from the bulk of ZnO (0002) film is vanishing, *ss*-SHG can be used to reveal sensitively the planar defects developed in the film. However, it is difficult to deduce qualitatively how  $\chi_{ijk}^{(2),m}$  varies with the generation of twin boundaries. Notice that the stress of ZnO (0002) thin film estimated from XRD decreases with increasing substrate temperature. The stress appearing at the ZnO film and substrate shall be the major contribution to the amplitude of  $\chi_{ijk}^{(2),m}$ .

Figure 2 exhibits an asymmetric two-lobed pattern, which does not agree with the symmetrical two-lobed pattern described by Eq. (1). One plausible reason to generate the asymmetrical two-lobed pattern is that the twin boundary does not have a mirror symmetry instead, the two planes relatively shift along the twin boundary.<sup>7</sup> The mirror structure with forward-backward symmetry is therefore broken. The second-order susceptibility can be modified by the stress gradient, which is properly described with a parameter *a*. Equation (1) then becomes

$$I_{s \rightarrow s}^{(2),m} \propto |\cos \phi (\cos^2 \phi \chi_{xxx}^{(2),m} + 2 \sin^2 \phi \chi_{xyy}^{(2),m}) + a|^2. \quad (2)$$

The theoretical curves (solid lines) based on Eq. (2) agree well with the experimental measured data shown in Fig. 2. From the fit, we found that  $\chi_{xxx}^{(2),m}$  reveals a mirror plane with nonlinear optical polarization perpendicular to  $[11\bar{2}0]$ , supporting the notion that the measured *ss*-RHG is caused by a planar defect.

The measured results with SHG are in fact averaged over the irradiated spot (10 mm<sup>2</sup>) and shall cover many domains. It is therefore surprising to discover that the measured azimuthal patterns of RSHG shown in Fig. 2 exhibit twofold symmetry, a result that has not been observed before in other studies. The nonzero polarity produced by the appearance of the plane defects between the neighboring twinned ZnO crystal domains related to the residual stress. This leads to the observed relation between *ss*-SHG and the residual stress in the films.

This work was supported from the National Science Council of the Republic of China under Contract Nos. NSC95-2112-M-415-002- and NSC 96-2112-M-415-004-.

- <sup>1</sup>F. C. M. Van De Pol, *Ceram. Bull.* **69**, 1959 (1990).
- <sup>2</sup>D. C. Look, D. C. Reynolds, J. R. Sizelove, R. L. Jones, C. W. Litton, G. Cantwell, and W. C. Harsch, *Solid State Commun.* **105**, 399 (1998).
- <sup>3</sup>J. L. Zhao, X. M. Li, J. M. Bian, W. D. Yu, and X. D. Gao, *J. Cryst. Growth* **276**, 507 (2005).
- <sup>4</sup>Y. Zhang, G. Du, B. Zhang, Y. Cui, H. Zhu, and Y. Chang, *Semicond. Sci. Technol.* **20**, 1132 (2005).
- <sup>5</sup>Y. R. Ryu, S. Zhu, J. M. Wrobel, H. M. Jeong, P. F. Miceli, and H. W. White, *J. Cryst. Growth* **216**, 326 (2000).
- <sup>6</sup>J. Yin, Z. G. Liu, X. S. Wang, T. Zhu, and J. M. Liu, *J. Cryst. Growth* **220**, 281 (2000).
- <sup>7</sup>Y. Yan, M. M. Al-Jassim, M. F. Chisholm, L. A. Boatner, S. J. Pennycook, and M. Oxley, *Phys. Rev. B* **71**, 041309 (2005).
- <sup>8</sup>F. Oba, H. Ohta, Y. Sato, H. Hosono, T. Yamamoto, and Y. Ikuhara, *Phys. Rev. B* **70**, 125415 (2004).
- <sup>9</sup>H. W. K. Tom, T. F. Heinz, and Y. R. Shen, *Phys. Rev. Lett.* **51**, 1983 (1983).
- <sup>10</sup>C. V. Shank, R. Yen, and C. Hirlimann, *Phys. Rev. Lett.* **51**, 900 (1983).
- <sup>11</sup>O. A. Aktsipetrov, A. A. Fedyanin, E. D. Mishina, A. N. Rubtsov, C. W. van Hasselt, M. A. C. Devillers, and Th. Rasing, *Phys. Rev. B* **54**, 1825 (1996).
- <sup>12</sup>K. Y. Lo, *J. Phys. D* **38**, 3926 (2005).
- <sup>13</sup>G. Lüpke, *Surf. Sci. Rep.* **35**, 75 (1999).
- <sup>14</sup>J. Y. Huang, *Jpn. J. Appl. Phys., Part 1* **33**, 3878 (1994).
- <sup>15</sup>D. J. Bottomley, A. Mito, P. J. Fons, S. Niki, and A. Yamada, *IEEE J. Quantum Electron.* **33**, 1294 (1997).
- <sup>16</sup>I. L. Lyubchanskii, N. N. Dadoenkova, M. I. Lyubchanskii, Th. Rasing, Jae-Woo Jeong, and Sung-Chul Shin, *Appl. Phys. Lett.* **76**, 1848 (2000).
- <sup>17</sup>K. Y. Lo, Y. J. Huang, J. Y. Huang, Z. C. Feng, W. E. Fenwick, M. Pan, and I. T. Ferguson, *Appl. Phys. Lett.* **90**, 161904 (2007).
- <sup>18</sup>K. Y. Lo and Y. J. Huang, *Phys. Rev. B* **76**, 035302 (2007).
- <sup>19</sup>V. Gupta and A. Mansingh, *J. Appl. Phys.* **80**, 1063 (1996).
- <sup>20</sup>H. P. He, F. Zhuge, Z. Z. Ye, L. P. Zhu, F. Z. Wang, B. H. Zhao, and J. Y. Huang, *J. Appl. Phys.* **99**, 023503 (2006).
- <sup>21</sup>Ü. Özgür, Ya. I. Alivov, C. Liu, A. Teke, M. A. Reshchikov, S. Doğan, V. Avrutin, S.-J. Cho, and H. Morkoç, *J. Appl. Phys.* **98**, 041301 (2005).
- <sup>22</sup>P. Bhattacharya, *Semiconductor Optoelectronic Devices* (Prentice Hall, New Jersey, 1997), Chap. 1.
- <sup>23</sup>W. Borchardt-Ott, *Crystallography* (Springer, New York, 1995), Chap. 13.
- <sup>24</sup>A. Yariv and P. Yeh, *Optical Waves in Crystals* (Wiley, New York, 1984), Chap. 12.